1-1-2015

Fusion analysis of first episode depression: where brain shape deformations meet local composition of tissue.

Mahdi Ramezani
Department of Electrical and Computer Engineering, The University of British Columbia, 2329 West Mall, Vancouver, BC V6T 1Z4, Canada

Purang Abolmaesumi
Department of Electrical and Computer Engineering, The University of British Columbia, 2329 West Mall, Vancouver, BC V6T 1Z4, Canada

Amir Tahmasebi
Philips Research North America, 345 Scarborough Rd., Briarcliff Manor, NY 10510, USA

Rachael Bosma
Department of Psychology, Queen's University, Kingston, ON K7L 3N6, Canada ; Centre for Neuroscience Studies, Queen's University, Kingston, ON K7L 3N6, Canada

Ryan Tong
Department of Psychology, Queen's University, Kingston, ON K7L 3N6, Canada

See next page for additional authors

NeuroImage: Clinical 7 (2015) 114–121

Contents lists available at ScienceDirect

NeuroImage: Clinical

journal homepage: www.elsevier.com/locate/ynicl

Fusion analysis of first episode depression: Where brain shape deformations meet local composition of tissue

Mahdi Ramezani[a,*], Purang Abolmaesumi[a], Amir Tahmasebi[b], Rachael Bosma[c,d], Ryan Tong[c], Tom Hollenstein[c,d], Kate Harkness[c,d], Ingrid Johnsrude[c,d,e]

[a]Department of Electrical and Computer Engineering, The University of British Columbia, 2329 West Mall, Vancouver, BC V6T 1Z4, Canada
[b]Philips Research North America, 345 Scarborough Rd., Briarcliff Manor, NY 10510, USA
[c]Department of Psychology, Queen's University, Kingston, ON K7L 3N6, Canada
[d]Centre for Neuroscience Studies, Queen's University, Kingston, ON K7L 3N6, Canada
[e]Department of Behavioural Sciences and Learning, Linnaeus Centre for Hearing and Deafness, Linköping University, Linköping SE-581 83, Sweden

ARTICLE INFO

Article history:
Received 21 August 2014
Received in revised form 9 November 2014
Accepted 23 November 2014
Available online 27 November 2014

Keywords:
Depression
Structural MRI
Joint analysis
Brain shape deformations
Brain local composition of tissue

ABSTRACT

Computational neuroanatomical techniques that are used to evaluate the structural correlates of disorders in the brain typically measure regional differences in gray matter or white matter, or measure regional differences in the deformation fields required to warp individual datasets to a standard space. Our aim in this study was to *combine* measurements of regional tissue composition and of deformations in order to characterize a particular brain disorder (here, major depressive disorder). We use structural Magnetic Resonance Imaging (MRI) data from young adults in a first episode of depression, and from an age- and sex-matched group of non-depressed individuals, and create population gray matter (GM) and white matter (WM) tissue average templates using DARTEL groupwise registration. We obtained GM and WM tissue maps in the template space, along with the deformation fields required to co-register the DARTEL template and the GM and WM maps in the population. These three features, reflecting tissue composition and shape of the brain, were used within a joint independent-components analysis (jICA) to extract spatially independent joint sources and their corresponding modulation profiles. Coefficients of the modulation profiles were used to capture differences between depressed and non-depressed groups. The combination of hippocampal shape deformations and local composition of tissue (but neither shape nor local composition of tissue alone) was shown to discriminate reliably between individuals in a first episode of depression and healthy controls, suggesting that brain structural differences between depressed and non-depressed individuals do not simply reflect chronicity of the disorder but are there from the very outset.

1. Introduction

Our understanding of the brain basis of psychiatric disorders, including Major Depressive Disorder (MDD), has benefited greatly over the past two decades from important advances in Magnetic Resonance Imaging (MRI) technology. Studies of adults with primarily recurrent episodes of MDD have shown significant volumetric differences in temporal (e.g., superior temporal gyrus [STG], hippocampus, amygdala) and frontal (e.g., anterior cingulate cortex [ACC] and orbitofrontal cortex [OFC]) brain regions relative to healthy controls (see Bellani et al., 2010; Bellani et al., 2011; Lorenzetti et al., 2009 for reviews of the neuroanatomy and structural MRI findings associated with MDD). The most consistent finding in these studies is reduced hippocampal volume in adult patients with MDD compared to healthy controls. However, some studies have also failed to find group differences in hippocampal volumes (Hastings et al., 2004; Monkul et al., 2007; Rusch et al., 2001; Vythilingam et al., 2004), and others have even reported larger hippocampal volumes in patients with MDD relative to healthy controls (Frodl et al., 2002; Vakili et al., 2000; Vythilingam et al., 2004).

A large number of approaches have been developed to characterize differences, among individuals and groups, in the neuroanatomical configuration of the human brain. Generally, these approaches are classified

* Corresponding author at: Robotics and Control Laboratory, Department of Electrical Engineering, The University of British Columbia, 2332 Main Mall, Vancouver, BC V6T 1Z4, Canada. Tel.: 604 366 1077; fax: 613 822 5942.
E-mail address: mahdir@ece.ubc.ca (M. Ramezani), purang@ece.ubc.ca (P. Abolmaesumi), amir.tahmasebi@philips.com (A. Tahmasebi), rachaelbosma@gmail.com (R. Bosma), 5rpt@queensu.ca (R. Tong), tom.hollenstein@queensu.ca (T. Hollenstein), harkness@queensu.ca (K. Harkness), ingrid.johnsrude@queensu.ca (I. Johnsrude).

http://dx.doi.org/10.1016/j.nicl.2014.11.016

into those that measure differences in brain shape, and those that measure differences in the local volume (and concentration) of brain tissue after macroscopic differences in shape have been discounted (Ashburner and Friston, 2000). The former approaches analyze the deformation fields required to map individual brains onto some standard reference in order to characterize neuroanatomy. Deformation Based Morphometry (DBM) (Bookstein, 1996) and Tensor Based Morphometry (TBM) (Chung et al., 2001) are widely used approaches that use deformation fields. Shape-analysis methods that are related to DBM/TBM have been widely employed to examine morphometric differences in depression. For example, in MDD, Posener et al. (2003) used high dimensional brain mapping on MRI data to quantitatively characterize the shape and volume of the hippocampus in adults with MDD and healthy controls (mean age $= 33 \pm 10$). They found significant group differences in hippocampal shape, but no evidence for differences in volume. In a more recent study, Zhao et al. (2008) applied SPherical HARMonic (SPHARM) shape analysis to the left and right hippocampi of elderly patients with MDD (age > 60) and healthy controls. Analysis revealed significant shape differences in the mid-body of the left hippocampus between the two groups. Further, patients in a current episode of MDD had lower left hippocampal volumes in comparison to controls, whereas patients in remission (Hawley et al., 2002) from MDD showed no reduction in hippocampal volume. In our previous study (Ramezani et al., 2014), we used multi-object statistical pose and shape analysis, and demonstrated brain morphological differences between adolescents with early-onset MDD and healthy controls.

Approaches that focus on the local composition of brain tissue, such as voxel-based morphometry (VBM), compare tissue images on a voxel-by-voxel basis after the deformation fields have been used to spatially normalize the images. For example, Bell-McGinty et al. (2002) applied VBM using SPM99, and reported smaller gray-matter volume of the right hippocampus, and smaller white-matter volume in the left anterior cingulate and right middle frontal gyrus, in elderly patients with MDD compared to healthy controls. Using VBM in SPM5, Vasic et al. (2008) reported significantly lower left hippocampal volumes in middle-aged patients with MDD in comparison to healthy controls. Similarly, in the same group of middle-aged patients with MDD, Bergouignan et al. (2009) compared VBM using a manual segmentation method and the automated method, and found significant hippocampal volume reductions using both segmentation methods in comparison with healthy controls. Finally, studies focusing on younger age groups, and including relevant covariates (i.e., age, sex, and intracranial volume) have also reported significantly lower hippocampal volumes, particularly in the left hemisphere, in both adolescents with MDD (MacMaster and Kusumakar, 2004) and in patients with early onset MDD and a family history of depression (MacMaster et al., 2008).

In summary, computational neuroanatomical techniques either use the deformation fields themselves to characterize brain structural variation, or use these fields to normalize images that are then entered into an analysis of regionally specific differences in tissue composition. Ideally, a procedure like VBM should be able to automatically identify any structural abnormalities in a single brain image. However, even with many hundreds of subjects in a database, the method may not be powerful enough to detect subtle abnormalities (Ashburner and Friston, 2000). Recently, unified voxel- and tensor-based morphometry (UVTM) that uses locally adaptive combination of TBM and VBM to improve sensitivity is proposed (Khan et al., 2014). UVTM is an extension of the Jacobian modulated VBM (Davatzikos et al., 2001), which gives weights to VBM or TBM analysis based on registration confidence. In modulated VBM, voxel concentration is scaled based on the amount of deformation which was applied in the registration procedure. Although the motivation for multiplying the Jacobian determinant of transformations and the tissue segmentation probabilities is intuitive, it is not clear if the statistically significant regions resulting from VBM and TBM will match, although it is assumed to be. In addition, there has been no quantitative study on determining the optimal weight parameters based on the registration confidence. A more powerful procedure would be to use a voxel-wise multivariate approach. Within a multivariate framework, in addition to images of gray matter concentration, other image features such as white matter concentration, and the deformation fields calculated during the spatial normalization procedure, can also be included (Ashburner and Friston, 2000). Fusion of these multiple images may help in detecting subtle individual differences.

Joint independent components analysis (jICA) (Calhoun et al., 2006a) is a multivariate technique for such "fusion analysis". It is an extension of independent-components analysis (ICA) that combines information from multiple features, which are a lower-dimensional representation of selected brain structures. jICA, as a group-level analysis technique, uses extracted features from individual subjects' data and tries to maximize the independence among joint components. jICA and extensions have been successfully applied to combine multimodal functional and structural images to study major depression (Choi et al., 2008), aphasia (Specht et al., 2009) and schizophrenia (Calhoun et al., 2006a; Calhoun et al., 2006b; Sui et al., 2009; Sui et al., 2010; Xu et al., 2009). For example, Choi et al. (2008) combined resting-state functional-connectivity and fractional-anisotropy data within jICA in a dataset of four subjects with MDD and nine healthy control subjects to investigate links between functional connectivity changes and white-matter abnormalities. They reported differences in the strength of connectivity and in the coherence of white-matter tracts among the subgenual anterior cingulate cortex (sACC) and perigenual ACC, anterior midcingulate cortex, caudate, thalamus, medial frontal cortex, amygdala, hippocampus, insula, and lateral temporal lobe.

The purpose of the current study was to combine, for the first time, brain shape and regional brain tissue composition using multivariate jICA in order to investigate the brain structural correlates of first-episode MDD. We determined the joint variation of shape and tissue composition in the hippocampal region in a sample of young people suffering from a first episode of MDD in comparison to a sample of young healthy controls. The importance of a young first-episode group is that they have not been subject to the known neurotoxic effects of glucocorticoids resulting from aging and the pathology of chronic depression (Sapolsky, 2000; Schuff et al., 1999). We hypothesize that, whereas conventional univariate analysis may not be sensitive to subtle differences in brain structure in this group, a multivariate technique that jointly analyzes multiple brain characteristics (i.e., shape and tissue composition) may have the requisite sensitivity to capture group differences. Following a group-wise registration using DARTEL (Ashburner, 2007; Bergouignan et al., 2009) to create an average template, we obtained individual gray-matter (GM) and white-matter (WM) tissue maps in the template space, along with the deformation fields required to co-register the template and the GM and WM maps. Using the jICA technique, we combined these three features, reflecting the tissue composition and shape of the brain in each individual, in order to extract spatially independent joint sources and their corresponding modulation profiles. We hypothesize that the mixing coefficients of the modulation profiles will lead to better discrimination of MDD subjects from the control group compared to the results obtained when brain shape and tissue composition are analyzed separately.

2. Material

2.1. Participants

Eleven young people with MDD (age: 18 ± 0.89, range: 16–21, 2 males, all right-handed) were recruited through referrals from community mental health clinics and through advertisement in a small city in Ontario, Canada. Fourteen healthy control subjects (all 18 years old; all female, all right-handed) were recruited through advertisement. The groups were well matched in age. There were no socioeconomic status (SES) differences between the subjects in the two groups

(p-value = 0.50). All subjects in the depressed group met the Diagnostic and Statistical Manual of Mental Disorders (DSM-IV-TR; American Psychiatric Association, 2000) criteria for a current episode of major depressive disorder based on the Structured Clinical Interview for DSM-IV Axis I Disorders (First et al., 1996) administered by an advanced doctoral student in clinical psychology. We used the Child and Adolescent version of the Schedule for Affective Disorders and Schizophrenia; K-SADS (Kaufman and Schweder, 2004). The K-SADS is the gold standard for DSM-IV diagnosis in children and adolescents and is the most widely used measure for this purpose in clinical research. Subjects were excluded if they met current or lifetime criteria for bipolar disorder, a psychotic disorder, a developmental disability (e.g., autism spectrum disorder), or a medical disorder that could cause depression (e.g., hypothyroidism). All participants in the MDD group were in their very first episode and were medication-free. This is important because understanding neuroanatomical features that characterize the earliest stages in the course of MDD, not confounded with medication use or recurrent MDD pathology, may provide important clues as to the disorder's initial etiology. All subjects in the depressed group had moderate to severe levels of symptoms, as defined by a score of 19 or greater on the Beck Depression Inventory (BDI-II (Beck et al., 1996)). The BDI is a 21-item self-report questionnaire that is the most common way to assess the presence and severity of depressive symptoms in adolescent and adult samples. Healthy controls had no current or past history of any psychiatric disorder and all had BDI scores of zero. We chose not to include the Hamilton Depression Rating Scale and to focus exclusively on the BDI as an index of depression severity since there is evidence that the Hamilton possesses a poor psychometric profile (Bagby et al., 2004). This study was cleared by the Health Sciences Research Ethics Board of Queen's University, and written informed consent was obtained from all participants, and from a parent or guardian for those participants under the age of 18.

2.2. Image acquisition

The MRI data were acquired using a 3.0 Tesla Siemens Trio MRI scanner with a 12-channel head coil in the MRI facility at Queen's University, Kingston, Canada. A whole-brain 3D MPRAGE T1-weighted anatomical image was acquired for each participant (voxel resolution of $1.0 \times 1.0 \times 1.0$ mm^3, flip angle $\alpha = 9°$, TR = 1760 ms, and TE = 2.6 ms).

3. Methods

In the following two subsections, first the input features to the jICA method, representing tissue composition and deformation of selected brain structures, are described. Then, the multivariate joint independent-components analysis technique, used to fuse multiple features, is briefly reviewed.

3.1. Features

The data type on which we focus in this paper is structural MRI (sMRI). Outcome measures derived from structural images include measures of shape (e.g., deformation) and tissue volume or concentration (e.g., gray or white matter). Below, we describe how we extracted three different features: (1) shape deformation information, and (2) gray- and (3) white-matter concentrations used for voxel-based morphometric (VBM) analysis.

The sMRI data were preprocessed using Statistical Parametric Mapping software (SPM8, Wellcome Department of Cognitive Neurology, London, UK). Briefly, GM, WM, and cerebral spinal fluid (CSF) were segmented using the automated segmentation processes in SPM (Ashburner, 2007; Bergouignan et al., 2009). This resulted in a set of three images in native space, in which each voxel is assigned a probability of being one of the three tissue types. The GM and WM maps were registered using the DARTEL method, which achieves accurate inter-subject registration of images (Ashburner, 2007; Bergouignan et al., 2009). The DARTEL procedure uses the GM and WM maps to create new templates and warps the GM and WM maps of each subject to the DARTEL template. Using DARTEL group-wise registration, the inter-subject registration is more accurate comparing to other SPM tools, therefore less spatial smoothing can be performed. We have used a Gaussian convolution kernel with a Full Width at Half Maximum (FWHM) of 8 mm. To demonstrate the effect of smoothing, we report the results with and without spatial smoothing. The deformation fields (DFs) required for warping the groupwise (DARTEL) template to the GM and WM maps of each subject were also created. These deformation fields show how much the group template structure deviates from each participant's structure. The absolute value of the deformation field (displacement) for each voxel is used to represent shape morphometry. The warped GM and WM segments along with the deformation fields are input features to the joint analysis method.

To reduce the number of voxels in the analysis, a segmented LPBA40/SPM5 atlas (Shattuck et al., 2008) in MNI space was used to extract the anatomical regions of interest. We selected the hippocampal region since abnormalities in this region have been associated with the pathology of MDD (Bellaniet al., 2010; Bellani et al., 2011; Lorenzetti et al., 2009). To account for small errors in the atlas-to-subject registration, the selected region was dilated using a disk with the radius of 5 voxels, with morphological operators to include adjacent regions in addition to the selected brain structure. Voxels inside the created mask were selected for joint analysis.

3.2. Joint independent-components analysis

We assume that there is a relation between brain tissue type (GM or WM) differences and brain structural deformations. This is not an unreasonable premise: if depression is associated with differences in both the size and shape of brain structures, then differences in the volume and/or concentration of gray and/or white matter might be related to differences in structural deformations in depressed individuals relative to controls. The three features described in the previous section were used as input observations ($X = [x_1, x_2, \ldots, x_N]^T \in R^{N \times K}$) to jICA in order to combine brain shape deformations and local composition of tissue. jICA can be used to identify any joint set of features ($S = [s_1, s_2, \ldots, s_N]^T \in R^{K \times N}$) that is anatomically differentiable between depressed subjects and healthy controls, where x_i ($i = 1, 2, \ldots, N$) is the vector of stacked features for subject i, and s_i shows the ith joint independent component (source). N is the number of subjects and K is the total dimensionality of stacked vectors. Considering the generative model $X = AS$, the aim of the jICA method is to find the matrix $W = A^{-1}$ so that the estimation of $U = WX$ is close to S. In this model, A is the matrix of mixing coefficients (also called ICA loading parameters, or the modulation profile), and W is the unmixing matrix. A MATLAB implementation of jICA is provided by the FIT 2.0b software (Calhoun et al., 2006a), available online at http://mialab.mrn.org/software/. A schematic of the jICA approach is shown in Fig. 1.

Joint independent components were found using the Infomax algorithm (Bell and Sejnowski, 1995), which is based on minimization of mutual information of components. In this algorithm, the output entropy of a neural network is adaptively maximized with as many outputs as the number of independent components (ICs) to be estimated. In order to use ICA, it is necessary to first specify the number of independent components (ICs) expected. We first attempted to estimate the number of ICs using the Minimum Description Length (MDL) criterion, which is an information-theoretic technique for model order selection (Li et al., 2007). Using the MDL criterion, the number of components in GM and WM was estimated to be 4 and 3, respectively, but because of the heterogeneity in the location and extent of deformations across both groups, this information-theoretic criterion did not converge for the deformation-field dataset. Accordingly, we instead follow the precedent set by Specht et al. (2009) and set the number of ICs equal to 1/3 of

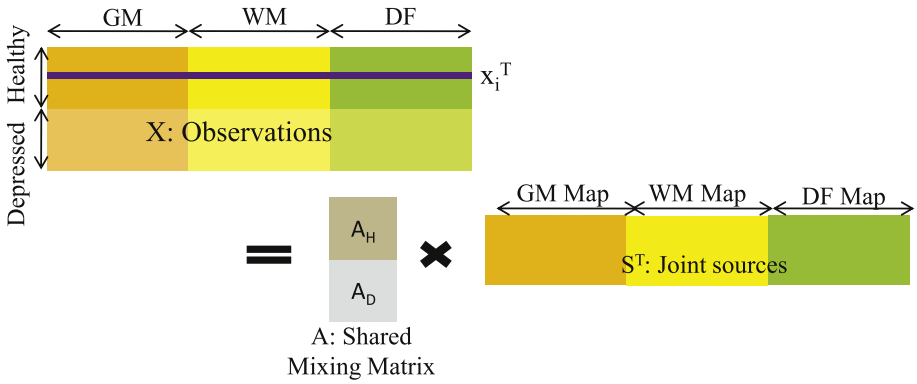

Fig. 1. Schematic of the jICA method. The observation matrix is made by stacking the GM, WM, and DF maps side by side. jICA tries to maximize the independence among maps of joint sources, assuming that they share the same mixing coefficient matrix.

the total number of subjects: so for 25 subjects here, we specify eight components.[1]

Separability of the mixing coefficients was used as a criterion for capturing group differences. These low-dimension coefficients reflect how much each subject's shape deformation and tissue composition are modulated by a joint source. To investigate whether the mixing coefficients truly differ between groups, we used two-sample (unpaired) t-tests. We report mixing coefficients that differ significantly between the two groups ($p < 0.05$), and for which the corresponding z-scaled component had more than 10 voxels with values above a threshold of $|z| > 2.5$ (99.4% cumulative probability). We followed the precedent set by Altena et al. (2010) to select minimum number of voxels within a cluster, and Sui et al. (2013) and Tosun et al. (2012) to select the threshold.

In order to determine whether the fusion analysis is superior (in terms of sensitivity) to analyses based on single features, we compared the result of t-tests on the mixing coefficients from the jICA of GM, WM and DF features to the result of the t-tests on each of the three features separately.

To further investigate the group differences, columns of the mixing coefficient matrix, which reflect the weighting of each joint source in a subject's GM, WM and DF, were used as input features to a classification algorithm. A discriminant analysis with a quadratic discriminant function was used to classify the subjects. Performance of the classifier was measured using leave-one-subject-out cross-validation, averaging classification performance across iterations. The joint ICA classification result was compared to classification results obtained with one or two features. The mixing coefficients were used as input features for the classification of depressed and control subjects.

Furthermore, separability of the joint source distributions was quantified by computing a divergence measure between joint histograms. Each of the joint sources was divided into three maps, which correspond to the GM, WM and deformation field features used in the jICA analysis. The map elements (each one representing a specific voxel) were thresholded and sorted in descending order by the voxel value, resulting in a set of voxels representing the greatest differences between groups in each joint source. For each subject, voxels that survived thresholding in all three maps were counted on a three-dimensional joint histogram in a bin defined by the three input feature values (from the input observation matrix *X* in Fig. 1) at those voxels' locations (see Calhoun et al., 2006b for more details on computing joint histograms). The group-averaged joint histograms were then calculated by taking the mean of the joint histograms across all the subjects in the group. The difference between the two groups was then assessed using the Renyi divergence formula (Hero et al., 2001). The divergence was also computed for other combinations of features (two or one). The higher the values of the Renyi divergence criterion, the better the discrimination between groups (Calhoun and Adali, 2009). The best combination of features is the one that yields the highest divergence value.

4. Results

We performed VBM analysis on GM and WM images obtained by DARTEL group-wise registration of the maps using the SPM8 toolbox. We used the same explicit mask (described in Subsection 3.1) that we had used for the joint ICA analysis of multiple features. Results show no significant WM, or GM differences using a Family Wise Error (FWE) rate of 0.05 or significance level of 0.001, and cluster size of 10 or more voxels.

We report the statistical difference among joint sources to evaluate the performance of the proposed joint analysis. Two-sample t-test was performed on the mixing coefficients, i.e., the eight columns of matrix A, which correspond to eight independent components, where each column consists of two groups of coefficients (one for each group of participants). One source differed significantly between the two groups ($p = 0.004$, which passed the Bonferroni correction for multiple comparisons ($p < 0.00625$)). Fig. 2(a) shows the mixing coefficients (i.e., weights) for this joint source, and its GM, WM and deformation-field components. The weights in the depressed group were significantly higher than in the control group. Fig. 2(b), (c) and (d) depicts the statistical Z maps around the left and right hippocampi (the regions of interest) for this joint source, and Table 1 shows the corresponding stereotaxic coordinates in MNI space. As can be seen in Fig. 2(d) and Table 1, the shape variations appear mostly in the left hemisphere of the brain within the hippocampal region, whereas group differences in the GM and WM concentrations appear in both hemispheres, as shown in Fig. 2(b) and (c). We remind the reader that for each subject, within the jICA framework, the coefficients that modulate the three maps (shape deformations and GM and WM concentrations within each joint source) are the same. In other words, the three maps, which represent the variation of shape deformations, and GM and WM concentrations among subjects, are jointly related. Hence, our results indicate that the statistically significant shape deformations observed within the left hemisphere of the brain in the hippocampal region are related to the statistically significant GM and WM alterations in the hippocampal region in both hemispheres. It is reasonable to infer from these results that local changes in brain tissue composition lead to alterations of shape in distant regions, because the brain is an interconnected organ.

[1] We performed subsequent follow-up analyses for 4, 10 and 12 components to further confirm the validity of our model and to test for the stability of the joint independent components. Stability analysis of the results for different numbers of independent components showed replication of findings for 10 and 12 independent components; however, using eight components yielded stronger group differences, and higher z-values. As expected (Ma et al., 2007), under-estimating the number of components (e.g., choosing four as the number of ICs in our case), yielded less reliable results. Results of analyses with 4, 10, and 12 ICs are available from the authors by request.

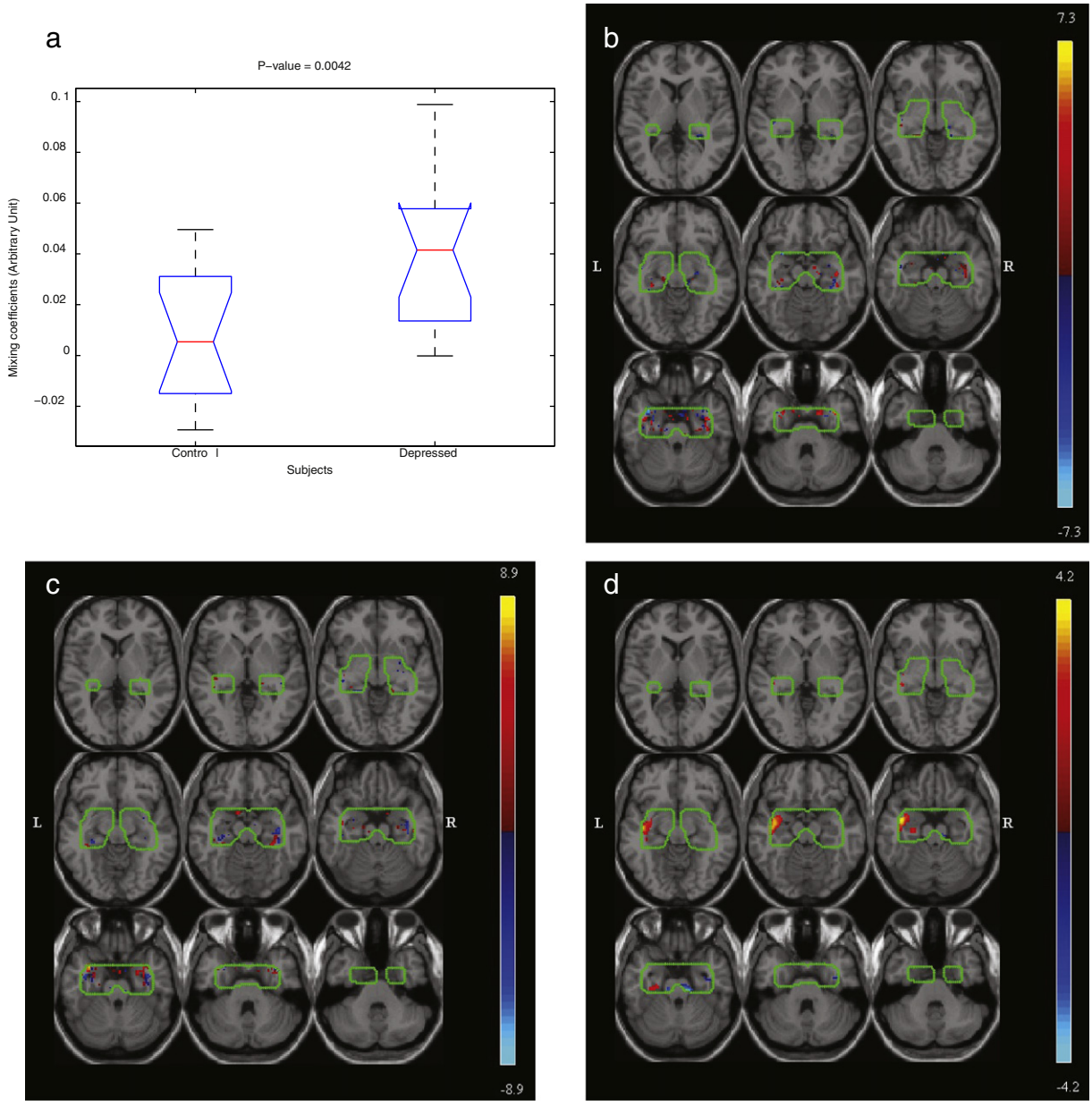

Fig. 2. Joint independent component analysis (jICA) of brain tissue composition and shape deformation. Panel (a) shows the mixing coefficients for the depressed and control subjects wherein the central red mark is the median, the edges of the blue box are the 25th and 75th percentiles, and the whiskers show the extreme values of the coefficients. Panels (b), (c), and (d) show the joint source map of the most significant component for (b) GM, (c) WM, and (d) deformation field. The green dots indicate the boundaries of the region of the interest which was created by dilating a mask around the hippocampus.

To determine the sensitivity of the fusion analysis in capturing the group differences, the results of joint analysis of GM + WM + DF, and of separate analysis of each of the GM, WM, and DF were compared. Eight independent-sample t-tests were conducted to compare depressed and non-depressed groups on the columns of the mixing coefficients for joint or separate analysis of features. The modulation profiles differed significantly between the two groups in the fusion analysis of GM + WM + DF features (Table 2). Results show that the combination of shape deformations and local composition of tissue, but neither shape nor local composition of tissue alone, can discriminate between individuals in the two groups. As it can be seen smoothing has not affected the results much.

Table 3 shows the average classification error for jICA (first column), and ICA (last three columns) of GM, WM, and DF, each used as input features in data fusion analysis. Results show that the control and depressed subjects can be classified based on structural MRI data with an error of 32% using the combination of shape deformations and tissue composition (GM + WM + DF). The classification error using shape deformations or tissue composition alone was more than 36%. Considering that the number of subjects is low and the dimensionality of the input MRI dataset is quite high, the results are very promising.

Fig. 3 shows the group-average marginal histograms for for GM, WM, and deformation fields, respectively. As can be seen, the histograms of the normalized intensity values for GM and WM were almost the same for the two groups, whereas the histogram of the absolute deformations showed around 0.3 mm more deformation for subjects with MDD compared to healthy controls.

The sorted maximum Renyi divergence values for different combinations of contrasts are shown in Fig. 4. Higher values indicate better discrimination between the groups. Therefore, as indicated in the figure, combining the deformation fields and tissue composition yielded greater discrimination than utilizing either deformation fields or tissue

Table 1
Stereotaxic coordinates for the most discriminative source map in three contrasts. MNI coordinates of voxels, which are above a threshold of |Z| > 2.5, and create a cluster volume of more than 10 voxels, are shown. L and R show the assigned anatomical left and right hemispheres, the coordinates and value of the maximum Z are also provided in the table. Not significant regions are shown by ns.

Feature	Volume (voxels)		Random effects: max value (x, y, z)	
	L	R	L	R
GM concentration				
Positive				
	69	55	5.5 (−33, −28, −12)	4.6 (33, −15, −18)
	44	74	5.0 (−39, −4, −26)	5.8 (33, 3, −30)
	26	30	4.3 (−30, 2, −27)	5.3 (35, −13, −27)
	23	9	5.0 (−41, −6, −26)	3.9 (38, −18, −26)
	4	19	3.9 (−29, −9, −18)	4.6 (35, −16, −17)
	2	18	6.4 (−39, −4, −27)	2.6 (38, −6, −29)
Negative				
	60	25	6.5 (−36, 3, −29)	4.0 (42, −13, −8)
	28	51	6.4 (−39, −36, −14)	5.0 (26, −39, −12)
	40	19	5.3 (−36, −37, −12)	4.5 (30, −33, −17)
	33	11	7.1 (−38, 6, −26)	5.1 (30, 8, −26)
	7	31	3.6 (−26, 8, −20)	4.1 (24, 0, −27)
WM concentration				
Positive				
	77	27	7.8 (−36, 3, −27)	5.1 (30, −3, −26)
	42	73	8.0 (−39, −36, −14)	6.6 (26, −39, −12)
	16	72	3.4 (−27, 2, −27)	5.0 (24, 0, −27)
	55	31	6.5 (−36, −37, −12)	5.8 (27, −39, −12)
	28	18	8.7 (−38, 6, −26)	6.2 (30, 8, −26)
Negative				
	61	91	6.1 (−39, −4, −26)	6.3 (33, 3, −29)
	80	86	6.6 (−33, −28, −12)	5.6 (33, −15, −18)
	30	15	6.2 (−41, −6, −26)	4.3 (42, −13, −24)
	18	1	7.8 (−39, −4, −27)	3.1 (38, −6, −27)
	2	16	4.5 (−33, −33, −9)	5.7 (35, −16, −17)
	13	11	5.2 (−30, 2, −27)	4.8 (33, −4, −27)
Deformation fields				
Positive				
	515	0	4.3 (−45, −5, −18)	ns
	13	0	2.6 (−32, −21, −24)	ns

composition data alone. In particular, combining GM and DF yielded the highest level of discriminatory power in both samples.

5. Discussion

The current study is the first to report that joint analysis of brain shape and tissue composition is sensitive enough to identify subtle, but reliable, differences between young people in a first episode of MDD and healthy controls. However, future work with larger datasets are required to confirm the superiority of the fusion analysis to separate analysis of shape and tissue composition. The identified corresponding sources demonstrate MDD-related links between WM, GM and shape deformation changes in the hippocampus, which were not detectable with univariate voxel-based methods. Assuming that the features share the same mixing coefficient matrix (modulation profile), jICA uses more information to estimate the same number of mixing

Table 2
p-Values of the most significant joint source, obtained from two-sample t-tests performed on the columns of the mixing coefficients generated by jICA (first columns), and ICA (last three columns). First and second rows show the results without and with spatial smoothing of the features. GM: gray matter; WM: white matter; DF: deformation field, each used as input features in data fusion analysis. The p-values displayed in the first column passed a Bonferroni correction for multiple comparison ($p < 0.00625$).

Smoothing \ Combination	GM + WM + DF	DF	GM	WM
None	0.004	0.069	0.067	0.081
FWHM: 8 mm	0.005	0.069	0.087	0.036

Table 3
Classification error obtained from discriminant analysis of the mixing coefficients generated by jICA (first column), and ICA (last three columns). GM: gray matter; WM: white matter; DF: deformation field, each used as input features in data fusion analysis.

Combination	GM + WM + DF	DF	GM	WM
Error	32%	36%	36%	40%

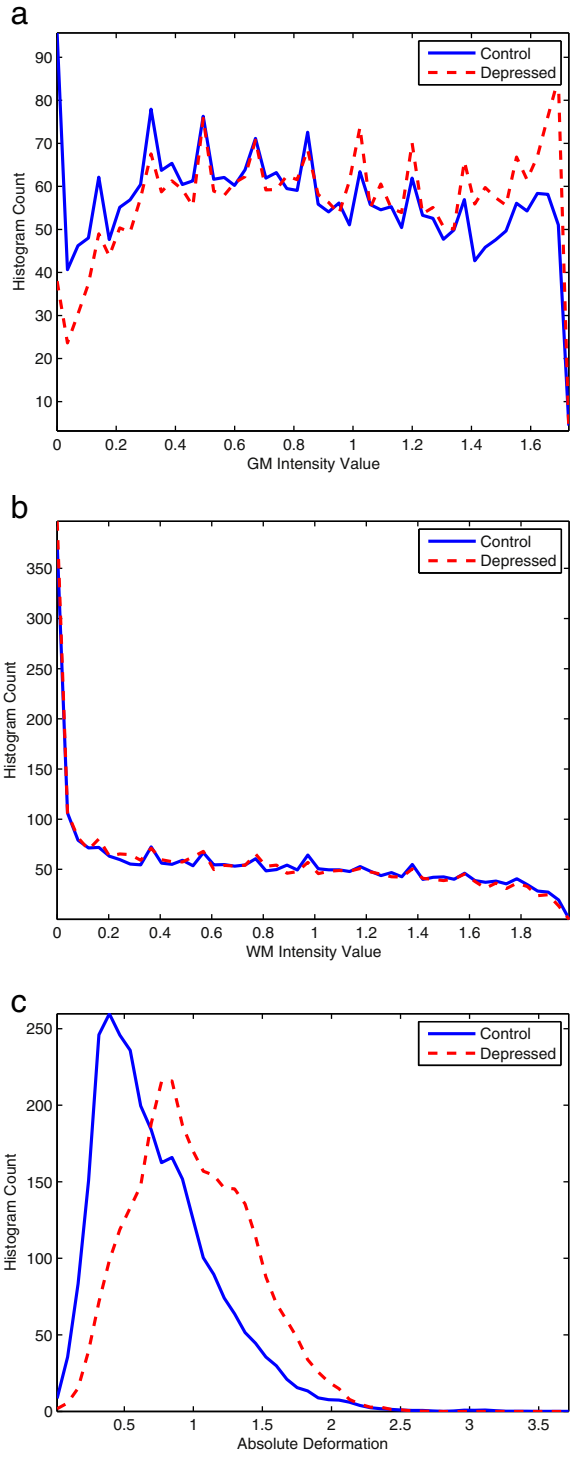

Fig. 3. Group-average histogram for the whole dataset on GM (a), WM (b), and deformation field (c). The difference between histograms of the two groups in deformation field was more than GM and WM.

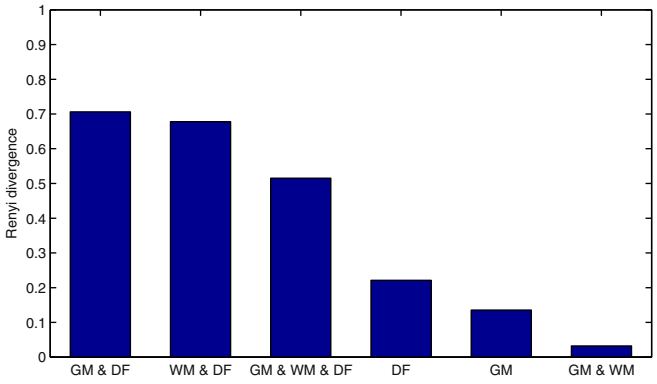

Fig. 4. Renyi divergence criteria values for different combination of features on differentiation between histograms. The first six highest value combinations are shown in the figure. The higher the values of the Renyi divergence, the better the discrimination between groups.

coefficients and may improve source estimations compared to ICA. The observed shape deformations in left hippocampus are related to GM and WM alterations in the hippocampus in both hemispheres (see Fig. 1 and Table 1). These significant shape deformation differences in the left hippocampus are consistent with a previous study of shape (Zhao et al., 2008), and volume differences (Vasic et al., 2008) in late-life MDD; and volume differences in adolescents with MDD (MacMaster and Kusumakar, 2004). Our results provide compelling evidence that shape-deformation differences in the hippocampus between depressed and healthy individuals are present to at least some extent even in the very initial stages of the illness; they do not simply emerge over the recurrent and chronic pathology of the disorder, and they are not simply the result of any potential neurotoxic effects of chronic anti-depressant usage.

Results demonstrate that individuals can be classified relatively accurately (with 68% accuracy) into control and depressed groups using only structural MRI data. This is consistent with previous attempts at the diagnostic classification of MDD using brain structural neuroanatomy (67.6% diagnostic accuracy reported by Costafreda et al., 2009 and 77.8% prognosis accuracy reported by Nouretdinov et al., 2011 using adult subjects). However, classification results reported using resting-state functional Magnetic Resonance Imaging are higher (94.3% reported by Zeng et al., 2012, 90.6% reported by Ma et al., 2013 and 95% reported by Craddock et al., 2009), suggesting that the analysis of cognitive functional differences may add considerable power to diagnostic classification in MDD.

The group-average histograms for individual features suggest that among individual features, the deformation fields may better discriminate the two groups. However, the combination of GM and deformation fields captured the group differences better than any individual feature alone, or any other combinations of features, as indicated by the values of the Renyi divergence. These results suggest that future studies should use both deformation fields, and regionally specific analyses, such as tissue composition measures, to better understand the brain basis of MDD and capture structural differences between individuals with MDD and healthy controls.

The results reported above should be interpreted in the context of the following limitations. First, this study comprised young women with moderate and severe depression almost exclusively; therefore, generalization to young men in a first episode of MDD, and young men and women with milder levels of depression severity requires further study. Second, we did not assess for the presence of comorbid anxiety disorders or specific subtypes of MDD. Future studies are required to examine variation in brain morphology with differing depression syndromes in order to identify biomarkers of more homogeneous endophenotypes. Third, it will be important in future research to determine whether the present results generalize to children and early adolescents with MDD, as significant corticolimbic plasticity remains throughout childhood and early adolescence (Giedd et al., 2010), which may obscure any potential toxic effects of depression vulnerability. Finally, the participants in this study were volunteers and, thus, may not be entirely representative of the population of young people with depression. Nevertheless, as a community sample, they may be more representative than the subjects of most previous studies, which have relied on treatment-seeking patients in tertiary care centers.

The proposed method based on fusion of brain-tissue composition and shape deformation successfully captured the differences in hippocampal shape and tissue composition between young people in a first episode of depression and healthy control subjects. Specifically, using the jICA method, significant shape deformation differences in the left hippocampus were observed between the depressed and control groups. In contrast, no differences were detected between the two groups when a separate analysis of each feature was conducted. These results suggest that the jICA method may be a more sensitive technique for detecting morphological differences in brain tissue — such sensitivity may be particularly helpful when the sample size is relatively small, or when structural abnormalities are relatively subtle (such as in groups of young people who are very early in their disease course). The current results have important clinical implications. Although prospective studies with individuals at risk for MDD are needed to determine the causal role of these structural differences in MDD, the current results suggest that hippocampal volume loss may be correlated for a particularly severe manifestation of MDD in the first onset.

Acknowledgments

The current study was supported by operating grants from the Canadian Institutes of Health Research (MOP-79320), and the Senate Advisory Research Committee of Queen's University (380327). The authors graciously acknowledge the technical assistance of Sharon David in helping with MRI image capture. The authors also wish to thank Jeremy Stewart, Kimberly Blom, and Lindsey Lytle for conducting the subject interviews.

References

Altena, E., Vrenken, H., Van Der Werf, Y.D., van den Heuvel, O.A., Van Someren, E.J., 2010. Reduced orbitofrontal and parietal gray matter in chronic insomnia: a voxel-based morphometric study. Biol. Psychiatry 67 (2), 182–185. http://dx.doi.org/10.1016/j.biopsych.2009.08.00319782344.

Ashburner, J., 2007. A fast diffeomorphic image registration algorithm. Neuroimage 38 (1), 95–113. http://dx.doi.org/10.1016/j.neuroimage.2007.07.00717761438.

Ashburner, J., Friston, K.J., 2000. Voxel-based morphometry — the methods. Neuroimage 11 (6 Pt 1), 805–821. http://dx.doi.org/10.1006/nimg.2000.058210860804.

Bagby, R.M., Ryder, A.G., Schuller, D.R., Marshall, M.B., 2004. The Hamilton Depression Rating Scale: has the gold standard become a lead weight? Am. J. Psychiatry 161 (12), 2163–2177. http://dx.doi.org/10.1176/appi.ajp.161.12.216315569884.

Beck, A.T., Steer, R.A., Ball, R., Ranieri, W., 1996. Comparison of Beck Depression Inventories-IA and -II in psychiatric outpatients. J. Pers. Assess. 67 (3), 588–597. http://dx.doi.org/10.1207/s15327752jpa6703_138991972.

Bell, A.J., Sejnowski, T.J., 1995. An information-maximization approach to blind separation and blind deconvolution. Neural Computation 7 (6), 1129–1159. http://dx.doi.org/10.1162/neco.1995.7.6.11297584893.

Bellani, M., Baiano, M., Brambilla, P., 2011. Brain anatomy of major depression II. Focus on amygdala. Epidemiology and Psychiatric Sciences 20 (1), 33–36. http://dx.doi.org/10.1017/S204579601100009621657113.

Bellani, M., Baiano, M., Brambilla, P., 2010. Brain anatomy of major depression I. Focus on hippocampus. Epidemiol. Psichiatr. Soc. 19 (4), 298–30121322503.

Bell-McGinty, S., Butters, M.A., Meltzer, C.C., Greer, P.J., Reynolds, C.F., Becker, J.T., 2002. Brain morphometric abnormalities in geriatric depression: long-term neurobiological effects of illness duration. Am. J. Psychiatry 159 (8), 1424–1427. http://dx.doi.org/10.1176/appi.ajp.159.8.142412153839.

Bergouignan, L., Chupin, M., Czechowska, Y., Kinkingnéhun, S., Lemogne, C., Le Bastard, G., Lepage, M., Garnero, L., 2009. Can voxel based morphometry, manual segmentation and automated segmentation equally detect hippocampal volume differences in acute depression? Neuroimage 45 (1), 29–37. http://dx.doi.org/10.1016/j.neuroimage.2008.11.00619071222.

Bookstein, F.L., 1996. Landmark methods for forms without landmarks: localizing group differences in outline shape. Math. Methods Biomed. Image Anal. 279–289.

Calhoun, V.D., Adali, T., Giuliani, N.R., Pekar, J.J., Kiehl, K.A., Pearlson, G.D., 2006a. Method for multimodal analysis of independent source differences in schizophrenia:

combining gray matter structural and auditory oddball functional data. Hum. Brain Mapp. 27 (1), 47–62. http://dx.doi.org/10.1002/hbm.2016616108017.
Calhoun, V.D., Adali, T., 2009. Feature-based fusion of medical imaging data. I. E.E.E. Trans. Inf. Technol. Biomed. 13 (5), 711–720. http://dx.doi.org/10.1109/TITB.2008.923773192730 16.
Calhoun, V.D., Adalı, T., Kiehl, K.A., Astur, R., Pekar, J.J., Pearlson, G.D., 2006b. A method for multitask fMRI data fusion applied to schizophrenia. Hum. Brain Mapp. 27 (7), 598–610. http://dx.doi.org/10.1002/hbm.20204.
Choi K., Craddock R.C., Holtzheimer P.E., Yang Z., Hu X., Mayberg H., A combined functional–structural connectivity analysis of major depression using joint independent components analysis. Proc. Intl. Soc. Mag. Reson. Med., 16 (2008). Psychiatric MRI/MRS, Toronto, Canada, p. 3555
Chung, M.K., Worsley, K.J., Paus, T., Cherif, C., Collins, D.L., Giedd, J.N., Rapoport, J.L., Evans, A.C., 2001. A unified statistical approach to deformation-based morphometry. Neuroimage 14 (3), 595–606. http://dx.doi.org/10.1006/nimg.2001.086211506533.
Costafreda, S.G., Chu, C., Ashburner, J., Fu, C.H., 2009. Prognostic and diagnostic potential of the structural neuroanatomy of depression. PLOS One 4 (7), e6353. http://dx.doi.org/10.1371/journal.pone.000635319633718.
Craddock, R.C., Holtzheimer, P.E., Hu, X.P., Mayberg, H.S., 2009. Disease state prediction from resting state functional connectivity. Magn. Reson. Med. 62 (6), 1619–1628. http://dx.doi.org/10.1002/mrm.2215919859933.
Davatzikos, C., Genc, A., Xu, D., Resnick, S.M., 2001. Voxel-based morphometry using the RAVENS maps: methods and validation using simulated longitudinal atrophy. Neuroimage 14 (6), 1361–1369. http://dx.doi.org/10.1006/nimg.2001.093711707092.
First, M., Gibbon, M., Spitzer, R., Williams, J., 1996. User's Guide for the Structured Clinical Interview for DSM-IV Axis I Disorders—Research Version. Biometrics Research Department, New York State Psychiatric Institute, New York.
Frodl, T., Meisenzahl, E.M., Zetzsche, T., Born, C., Groll, C., Jäger, M., Leinsinger, G., Bottlender, R., Hahn, K., Möller, H.J., 2002. Hippocampal changes in patients with a first episode of major depression. Am. J. Psychiatry 159 (7), 1112–1118. http://dx.doi.org/10.1176/appi.ajp.159.7.111212091188.
Giedd, J.N., Stockman, M., Weddle, C., Liverpool, M., Alexander-Bloch, A., Wallace, G.L., Lee, N.R., Lalonde, F., Lenroot, R.K., 2010. Anatomic magnetic resonance imaging of the developing child and adolescent brain and effects of genetic variation. Neuropsychol. Rev. 20 (4), 349–361. http://dx.doi.org/10.1007/s11065-010-9151-921069466.
Hastings, R.S., Parsey, R.V., Oquendo, M.A., Arango, V., Mann, J.J., 2004. Volumetric analysis of the prefrontal cortex, amygdala, and hippocampus in major depression. Neuropsychopharmacology 29 (5), 952–959. http://dx.doi.org/10.1038/sj.npp.130037114997169.
Hawley, C.J., Gale, T.M., Sivakumaran, T., 2002. Defining remission by cut off score on the MADRS: selecting the optimal value. J. Affect. Disord. 72 (2), 177–184. http://dx.doi.org/10.1016/S0165-0327(01)00451-712200208.
Hero, A.O., Ma, B., Michel, O., Gorman, J., 2001. Alpha-divergence for classification, indexing and retrieval. Communication and Signal Processing Laboratory, Technical Report CSPL-328. University of Michigan, Ann Arbor.
Kaufman, J., Schweder, A.E., 2004. The schedule for affective disorders and schizophrenia for school-age children: present and lifetime version. Comprehensive handbook of psychological assessment. J. Personal. Assess. 2, 247.
Khan, A.R., Wang, L., Beg, M.F., 2014. Unified voxel- and tensor-based morphometry (UVTBM) using registration confidence. Neurobiol. Aging S0197–S4580.
Li, Y.O., Adali, T., Calhoun, V.D., 2007. Estimating the number of independent components for functional magnetic resonance imaging data. Hum. Brain Mapp. 28 (11), 1251–1266. http://dx.doi.org/10.1002/hbm.2035917274023.
Lorenzetti, V., Allen, N.B., Fornito, A., Yücel, M., 2009. Structural brain abnormalities in major depressive disorder: a selective review of recent MRI studies. J. Affect. Disord. 117 (1-2), 1–17. http://dx.doi.org/10.1016/j.jad.2008.11.02119237202.
Ma, L., Wang, B., Chen, X., Xiong, J., 2007. Detecting functional connectivity in the resting brain: a comparison between ICA and CCA. Magn. Reson. Imaging 25 (1), 47–56. http://dx.doi.org/10.1016/j.mri.2006.09.03217222714.
Ma, Q., Zeng, L.L., Shen, H., Liu, L., Hu, D., 2013. Altered cerebellar–cerebral resting-state functional connectivity reliably identifies major depressive disorder. Brain Res. 1495, 86–94. http://dx.doi.org/10.1016/j.brainres.2012.12.00223228724.
MacMaster, F.P., Mirza, Y., Szeszko, P.R., Kmiecik, L.E., Easter, P.C., Taormina, S.P., Lynch, M., Rose, M., Moore, G.J., Rosenberg, D.R., 2008. Amygdala and hippocampal volumes in familial early onset major depressive disorder. Biol. Psychiatry 63 (4), 385–390. http://dx.doi.org/10.1016/j.biopsych.2007.05.00517640621.
MacMaster, F.P., Kusumakar, V., 2004. Hippocampal volume in early onset depression. B.M.C. Med. 2, 2. http://dx.doi.org/10.1186/1741-7015-2-214969587.
Monkul, E.S., Hatch, J.P., Nicoletti, M.A., Spence, S., Brambilla, P., Lacerda, A.L., Sassi, R.B., Mallinger, A.G., Keshavan, M.S., Soares, J.C., 2007. Fronto-limbic brain structures in suicidal and non-suicidal female patients with major depressive disorder. Mol. Psychiatry 12 (4), 360–366. http://dx.doi.org/10.1038/sj.mp.400191917389903.
Nouretdinov, I., Costafreda, S.G., Gammerman, A., Chervonenkis, A., Vovk, V., Vapnik, V., Fu, C.H., 2011. Machine learning classification with confidence: application of transductive conformal predictors to MRI-based diagnostic and prognostic markers in depression. Neuroimage 56 (2), 809–813. http://dx.doi.org/10.1016/j.neuroimage.2010.05.02320483379.
Posener, J.A., Wang, L., Price, J.L., Gado, M.H., Province, M.A., Miller, M.I., Babb, C.M., Csernansky, J.G., 2003. High-dimensional mapping of the hippocampus in depression. Am. J. Psychiatry 160 (1), 83–89. http://dx.doi.org/10.1176/appi.ajp.160.1.8312505805.
Ramezani, M., Johnsrude, I., Rasoulian, A., Bosma, R., Tong, R., Hollenstein, T., Harkness, K., Abolmaesumi, P., 2014. Temporal-lobe morphology differs between healthy adolescents and those with early-onset of depression. Neuroimage Clin. 6, 145–155. http://dx.doi.org/10.1016/j.nicl.2014.08.00725379426.
Rusch, B.D., Abercrombie, H.C., Oakes, T.R., Schaefer, S.M., Davidson, R.J., 2001. Hippocampal morphometry in depressed patients and control subjects: relations to anxiety symptoms. Biol. Psychiatry 50 (12), 960–964. http://dx.doi.org/10.1016/S0006-3223(01)01248-311750892.
Sapolsky, R.M., 2000. The possibility of neurotoxicity in the hippocampus in major depression: a primer on neuron death. Biol. Psychiatry 48 (8), 755–765. http://dx.doi.org/10.1016/S0006-3223(00)00971-911063972.
Schuff, N., Amend, D.L., Knowlton, R., Norman, D., Fein, G., Weiner, M.W., 1999. Age-related metabolite changes and volume loss in the hippocampus by magnetic resonance spectroscopy and imaging. Neurobiology of Aging 20 (3), 279–285. http://dx.doi.org/10.1016/S0197-4580(99)00022-610588575.
Shattuck, D.W., Mirza, M., Adisetiyo, V., Hojatkashani, C., Salamon, G., Narr, K.L., Poldrack, R.A., Bilder, R.M., Toga, A.W., 2008. Construction of a 3D probabilistic atlas of human cortical structures. Neuroimage 39 (3), 1064–1080. http://dx.doi.org/10.1016/j.neuroimage.2007.09.03118037310.
Specht, K., Zahn, R., Willmes, K., Weis, S., Holtel, C., Krause, B.J., Herzog, H., Huber, W., 2009. Joint independent component analysis of structural and functional images reveals complex patterns of functional reorganisation in stroke aphasia. Neuroimage 47 (4), 2057–2063. http://dx.doi.org/10.1016/j.neuroimage.2009.06.01119524049.
Sui, J., Adali, T., Pearlson, G.D., Clark, V.P., Calhoun, V.D., 2009. A method for accurate group difference detection by constraining the mixing coefficients in an ICA framework. Hum. Brain Mapp. 30 (9), 2953–2970. http://dx.doi.org/10.1002/hbm.2072119172631.
Sui, J., Adali, T., Pearlson, G., Yang, H., Sponheim, S.R., White, T., Calhoun, V.D., 2010. A CCA+ICA based model for multi-task brain imaging data fusion and its application to schizophrenia. Neuroimage 51 (1), 123–134. http://dx.doi.org/10.1016/j.neuroimage.2010.01.06920114081.
Sui, J., He, H., Yu, Q., Chen, J., Rogers, J., Pearlson, G.D., Mayer, A., Bustillo, J., Canive, J., Calhoun, V.D., 2013. Combination of resting state fMRI, DTI, and sMRI data to discriminate schizophrenia by N-way MCCA + jICA. Front. Hum. Neurosci. 7, 235. http://dx.doi.org/10.3389/fnhum.2013.0023523755002.
Tosun, D., Rosen, H., Miller, B.L., Weiner, M.W., Schuff, N., 2012. MRI patterns of atrophy and hypoperfusion associations across brain regions in frontotemporal dementia. Neuroimage 59 (3), 2098–2109. http://dx.doi.org/10.1016/j.neuroimage.2011.10.03122036676.
Vakili, K., Pillay, S.S., Lafer, B., Fava, M., Renshaw, P.F., Bonello-Cintron, C.M., Yurgelun-Todd, D.A., 2000. Hippocampal volume in primary unipolar major depression: a magnetic resonance imaging study. Biol. Psychiatry 47 (12), 1087–1090. http://dx.doi.org/10.1016/S0006-3223(99)00296-610862809.
Vasic, N., Walter, H., Höse, A., Wolf, R.C., 2008. Gray matter reduction associated with psychopathology and cognitive dysfunction in unipolar depression: a voxel-based morphometry study. J. Affect. Disord. 109 (1-2), 107–116. http://dx.doi.org/10.1016/j.jad.2007.11.01118191459.
Vythilingam, M., Vermetten, E., Anderson, G.M., Luckenbaugh, D., Anderson, E.R., Snow, J., Staib, L.H., Charney, D.S., Bremner, J.D., 2004. Hippocampal volume, memory, and cortisol status in major depressive disorder: effects of treatment. Biol. Psychiatry 56 (2), 101–112. http://dx.doi.org/10.1016/j.biopsych.2004.04.00215231442.
Xu, L., Pearlson, G., Calhoun, V.D., 2009. Joint source based morphometry identifies linked gray and white matter group differences. Neuroimage 44 (3), 777–789. http://dx.doi.org/10.1016/j.neuroimage.2008.09.05118992825.
Zeng, L.L., Shen, H., Liu, L., Wang, L., Li, B., Fang, P., Zhou, Z., Li, Y., Hu, D., 2012. Identifying major depression using whole-brain functional connectivity: a multivariate pattern analysis. Brain 135 (5), 1498–1507. http://dx.doi.org/10.1093/brain/aws05922418737.
Zhao, Z., Taylor, W.D., Styner, M., Steffens, D.C., Krishnan, K.R., MacFall, J.R., 2008. Hippocampus shape analysis and late-life depression. PLOS One 3 (3), e1837. http://dx.doi.org/10.1371/journal.pone.000183718350172.